Co-assembly of N-type Ca^{2+} and BK channels underlies functional coupling in rat brain

David J. Loane*, Pedro A. Lima‡ and Neil V. Marrion§

Department of Pharmacology and MRC Centre for Synaptic Plasticity, University of Bristol, Bristol, BS8 1TD, UK

*Present address: Laboratory for the Study of CNS Injury, Department of Neuroscience, Georgetown University Medical Center, Washington, DC 20057, USA

‡Present address: Dep. Fisiologia, Fac. Ciências Médicas, UNL, 1169-056 Lisboa, Portugal

§Author for correspondence (e-mail: N.V.Marrion@bris.ac.uk)

Accepted 9 January 2007
Journal of Cell Science 120, 985-995 Published by The Company of Biologists 2007
doi:10.1242/jcs.03399

Summary

Activation of large conductance Ca^{2+}-activated potassium (BK) channels hastens action potential repolarisation and generates the fast afterhyperpolarisation in hippocampal pyramidal neurons. A rapid coupling of Ca^{2+} entry with BK channel activation is necessary for this to occur, which might result from an identified coupling of Ca^{2+} entry through N-type Ca^{2+} channels to BK channel activation. This selective coupling was extremely rapid and resistant to intracellular BAPTA, suggesting that the two channel types are close. Using reciprocal co-immunoprecipitation, we found that N-type channels were more abundantly associated with BK channels than L-type channels ($Ca_V1.2$) in rat brain. Expression of only the pore-forming α-subunits of the N-type ($Ca_V2.2$) and BK (Slo_{27}) channels in a non-neuronal cell-line gave robust macroscopic currents and reproduced the interaction. Co-expression of $Ca_V2.2/Ca_V\beta_3$ subunits with Slo_{27} channels revealed rapid functional coupling. By contrast, extremely rare examples of rapid functional coupling were observed with co-expression of $Ca_V1.2/Ca_V\beta_3$ and Slo_{27} channels. Action potential repolarisation in hippocampal pyramidal neurons was slowed by the N-type channel blocker ω-conotoxin GVIA, but not by the L-type channel blocker isradipine. These data showed that selective functional coupling between N-type Ca^{2+} and BK channels provided rapid activation of BK channels in central neurons.

Key words: Co-immunoprecipitation, Channel coupling, Hippocampus, Action potential

Introduction

Membrane proteins can be organised into complexes with other proteins. There has been particular focus on the association of effector molecules with their targets. For example, the large conductance Ca^{2+}-activated potassium (BK) channel has been reported to be present in a large signalling complex in rat brain that includes the β_2 adrenergic receptor, the cytosolic A-kinase-anchoring protein (AKAP79), protein kinase A (PKA) and the L-type Ca^{2+} channel (Liu et al., 2004). Results such as this led to the idea that ion channels can reside and be modulated within a specialised membrane micro-domain (Davare et al., 1999; Liu et al., 2004).

Considerable evidence exists showing that ion channel subtypes may co-exist within membrane micro-domains. There have been a number of examples where Ca^{2+} ion entry through different channel types leads to activation of Ca^{2+}-activated channels. For example, activation of small conductance Ca^{2+}-activated (SK) channels within the CNS can result from Ca^{2+} entry through voltage-gated L-type (Marrion and Tavalin, 1998), T-type (Wolfart and Roeper, 2002), P-type (Edgerton and Reinhart, 2003) and N-type (Hallworth et al., 2003) Ca^{2+} channels. In addition, SK channel activation can arise from Ca^{2+} entry through NMDA receptors (Faber et al., 2005). Activation of BK channels can occur by Ca^{2+} entry through particular ion channel types. For example, it has been reported that Ca^{2+} entry through NMDA receptors (Isaacson and Murphy, 2001), voltage-dependent N-type (Marrion and Tavalin, 1998) or L- and N-type Ca^{2+} channels (Sun et al., 2003) can activate BK channels in different central neurons. It is likely that the identity of channel subtypes involved in functional coupling may vary according to cell type. In most cases, functional coupling has been inferred from the effects of block of a Ca^{2+} channel subtype on the activation of Ca^{2+}-activated current (Edgerton and Reinhart, 2003; Faber et al., 2005; Hallworth et al., 2003; Isaacson and Murphy, 2001; Sun et al., 2003; Wolfart and Roeper, 2002). These data fail to distinguish between functional coupling resulting from a specific interaction between channel subtypes and that arising because channels share the same subcellular location. A common subcellular location may be the case of functional coupling to the activation of SK channels, because these channels are more Ca^{2+} sensitive (Hirschberg et al., 1998; Xia et al., 1998) and require some distance between Ca^{2+} source and channel to experience the correct Ca^{2+} concentration for activation (Marrion and Tavalin, 1998). This is expected to be different for BK channels, as they are required to be closer to the source of Ca^{2+} entry because they are less sensitive to Ca^{2+} concentration than SK channels (Vergara et al., 1998). The BK channel must be extremely close to the source of Ca^{2+} because its activation has to occur <1 msecond to hasten the repolarisation of the action potential in hippocampal neurons (Lancaster and Nicoll, 1987; Storm, 1987). Three studies have identified a selective colocalisation of BK and Ca^{2+} channels: one using single-channel analysis that directly showed functional coupling of N-type and BK channels in hippocampal CA1 pyramidal neurons (Marrion and Tavalin, 1998) and two

using biochemical techniques to demonstrate the association of L-type and BK channels in rat whole brain (Grunnet and Kaufmann, 2004; Berkefeld et al., 2006). However, no study has yet identified the rapid functional coupling between BK and Ca^{2+} channels and resolved how this might be achieved.

We show that the functional coupling of N-type Ca^{2+} and BK channels in whole rat brain and hippocampus results from the co-assembly of the two proteins. This association was markedly more abundant than the association of L-type ($Ca_V1.2$) and BK channels in brain. Association of N-type Ca^{2+} ($Ca_V2.2$) and BK ($rSlo_{27}$) channels was reconstituted by expression of only the pore-forming α-subunits. Functional coupling between $Ca_V2.2$ and $rSlo_{27}$ channels expressed in tsA-201 cells was frequent and was observed to be identical to that seen in hippocampal neurons: a coupling that was resistant to the buffering of intracellular Ca^{2+} by BAPTA (Marrion and Tavalin, 1998). Coupled events were very rarely observed in tsA-201 cells expressing $Ca_V1.2$ and $rSlo_{27}$ subunits. In contrast to the block of L-type Ca^{2+} channels with isradipine, application of the N-type channel blocker ω-conotoxin GVIA to hippocampal slices slowed CA1 pyramidal cell action potential repolarisation, showing that the specific intimate association of channel pore-forming subunits permits the rapid activation of BK channels to hasten action potential repolarisation (Lancaster and Nicoll, 1987; Shao et al., 1999).

Results

N-type Ca^{2+} channels and BK channels co-assembled in rat brain

The functional coupling between N-type Ca^{2+} and BK channels identified in hippocampal CA1 neurons suggested a close association between channel subunits (Marrion and Tavalin, 1998). Co-immunoprecipitation (co-IP) from native rat brain using antibodies directed against the pore-forming α-subunits was performed to reveal whether interactions between channel subunits were responsible for functional coupling. Immunoblotting the anti-$BK\alpha_{1118\text{-}1135}$ co-IP (BK-IP) sample with an antibody directed against the N-type Ca^{2+} channel (anti-$Ca_V2.2$) revealed a strong immunoreactive band of the predicted molecular mass of the native $Ca_V2.2$ subunit (210 kDa) (Fig. 1Ai). Enrichment of BK channel α-subunit immunoreactivity in the BK-IP confirmed the specificity of the immunoprecipitation (Fig. 1Aii). This specificity of the interaction was further confirmed by the absence of the band corresponding to the $Ca_V2.2$ subunit in the control rabbit IgG co-IP (IgG-IP) (Fig. 1Ai).

Co-IP of channel proteins was also performed from rat hippocampal tissue, because functional colocalisation of N-type Ca^{2+} channels and BK channels was first demonstrated in hippocampal CA1 pyramidal neurons (Marrion and Tavalin, 1998). As observed for whole brain, a strong immunoreactive band of the predicted molecular mass of the native $Ca_V2.2$ subunit (~210 kDa) was detected in the BK-IP, but was absent in the control IgG-IP (Fig. 1B). Reciprocal co-immunoprecipitation experiments were performed using anti-$Ca_V2.2$ as the precipitating antibody. Immunoblotting the anti-$Ca_V2.2$ co-IP ($Ca_V2.2$-IP) with anti-BK revealed a strong band of the predicted molecular mass of the BK channel α-subunit, a band that was absent from the control rabbit IgG-IP (Fig. 1Ci). Enrichment of $Ca_V2.2$ immunoreactivity in the $Ca_V2.2$-IP indicated the specificity of the immunoprecipitation (Fig. 1Cii). These data demonstrated that N-type Ca^{2+} and BK channels are co-assembled in rat hippocampus and whole brain.

Co-assembly of N-type Ca^{2+} and BK channels with expression of pore-forming α-subunits

Co-immunoprecipitation of native brain channel proteins demonstrated that N-type Ca^{2+} and BK channels co-assemble to form a protein complex in rat brain. However, this approach cannot determine whether the interaction is direct, or requires other proteins present in brain. To circumvent this problem, we chose to express only the pore-forming α-subunits of each channel subtype in a non-neuronal cell-line (tsA-201) to determine whether association of channel subunits occurred with these 'minimal' channels.

It was imperative that functional channels were expressed under the conditions used to identify interaction between α-subunits. Transient transfection of tsA-201 cells with N-terminal GFP-$Ca_V2.2$ (GFP-$Ca_V2.2$) (Raghib et al., 2001) alone gave a voltage-dependent inward current (Fig. 2Ai) that was half activated at +21 mV (n=12) (Fig. 2Aii). Whole-cell currents exhibited voltage-dependent inactivation during the sustained depolarisation (Fig. 2Ai). Steady-state inactivation determined by a pre-pulse protocol (see Fig. 2, legend) was fit with a Boltzmann distribution, with a $V_{½}$ of –21 mV (n=10) (Fig. 2Aii). In addition, ~90% of current recorded in 60 mM Ba^{2+} was blocked by the N-type Ca^{2+} channel antagonist ω-conotoxin GVIA (300 nM) (data not shown). Inward currents were not observed in cells expressing EGFP alone. These properties were similar to currents recorded from HEK293 cells expressing $Ca_V2.2$ subunits alone (Yasuda et al., 2004; Butcher et al., 2006). Expression of $rSlo_{27}$ (Ha et al., 2000) gave Ca^{2+}-dependent and voltage-dependent whole cell and single channel currents. Whole-cell currents were observed only when cells were dialysed with 1 μM Ca^{2+} (Fig. 2Bi), with currents showing clear voltage dependence (Fig. 2Bi,ii). Excised inside-out patches exhibited Ca^{2+}-dependent channel activity of 217±17 pS (n=4) conductance (data not shown). Ca^{2+}-activated outward currents were not observed in cells expressing EGFP alone. $rSlo_{27}$ current activated at more negative voltages than seen when expressed in *Xenopus* oocytes (Ha et al., 2000): a property also observed when human and mouse Slo subunits were expressed in mammalian cell lines (Alioua et al., 2002; Ling et al., 2000). These data showed that expression of only the pore-forming α-subunits of each channel subtype gave functional current. GFP-$Ca_V2.2$ and $rSlo_{27}$ subunit expression was visualised by western immunoblotting with anti-BK or an antibody directed against the N-terminal GFP tag of the $Ca_V2.2$ subunit (anti-GFP). Co-IP with anti-GFP from tsA-201 cells co-transfected with GFP-$Ca_V2.2$ and $rSlo_{27}$ (GFP-IP) was probed with anti-BK to reveal a band of the predicted molecular mass of the $rSlo_{27}$ channel α-subunit protein (Fig. 2Ci). Probing the GFP-IP with either anti-GFP or anti-$Ca_V2.2$ showed two bands that were of the predicted molecular mass of GFP-$Ca_V2.2$ (Fig. 2Cii). This demonstrated that anti-GFP specifically immunoprecipitated GFP-$Ca_V2.2$ channel protein complexes from co-transfected tsA-201 cells. These data indicated that the α-subunits of each channel interacted in a non-neuronal cell-line and suggested that an interaction between α-subunits underlies association in brain (see below).

Functional coupling of N-type Ca^{2+} channels and BK channels reconstituted in tsA-201 cells

The observed co-assembly between channel α-subunits raised the question of whether this association could provide functional coupling between channel subtypes. Whole-cell current was observed in cells expressing GFP-$Ca_V2.2$ (Fig. 2A), but single channel currents could not be resolved. Co-expression of $Ca_V2.2$ and $Ca_V\beta_3$ subunits that are abundant in hippocampus (Sochivko et al., 2003), increased the amplitude of macroscopic current and shifted the voltage-dependence of activation to more negative potentials when compared with data obtained from expression of $Ca_V2.2$ subunits alone (Fig. 3A cf. Fig. 2A). This was consistent with the reported effects of co-expression of $Ca_V\beta_3$ subunits with $Ca_V2.2$ (Yasuda et al., 2004; Butcher et al., 2006). These data confirmed that the majority of macroscopic current recorded from cells expressing $Ca_V2.2$ alone was not derived from association with endogenous $Ca_V\beta$ subunits (Leroy et al., 2005). Co-expression of $Ca_V2.2$ and $Ca_V\beta_3$ subunits gave resolvable single channel currents (Fig. 3B) with a slope conductance of 8.4±0.08 pS (using 160 mM Ca^{2+}, n=3) and an open duration distribution best fit by a single exponential of time constant 1.1±0.09 mseconds at +20 mV (n=7).

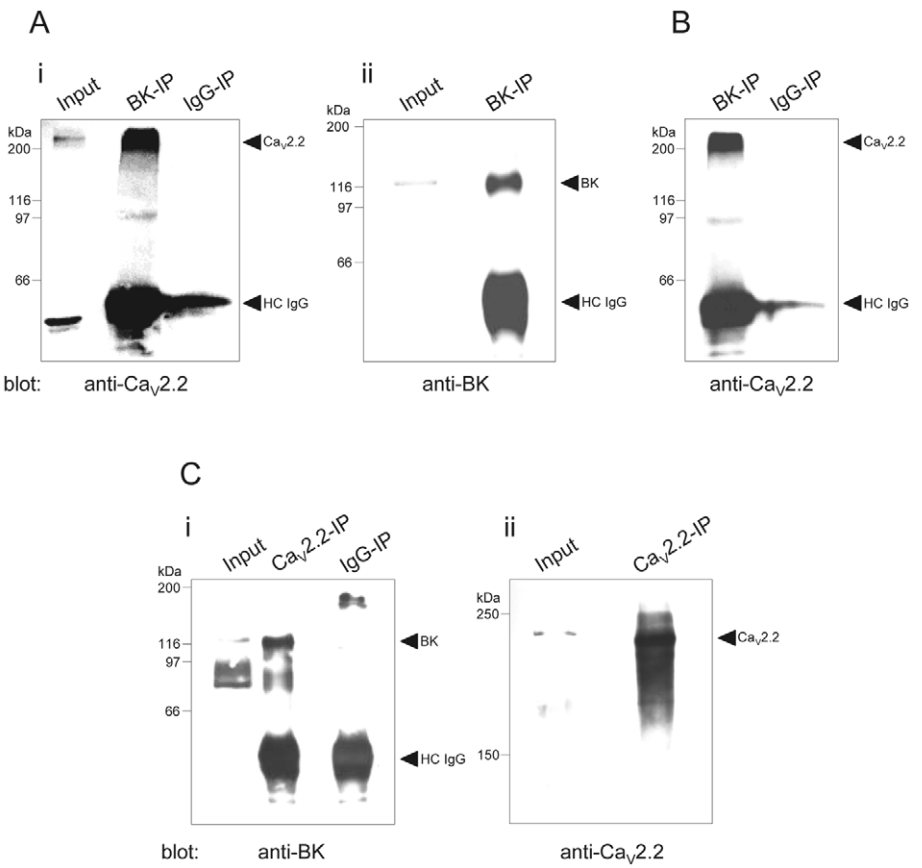

Fig. 1. Reciprocal co-immunoprecipitation from rat brain and hippocampus demonstrated selective co-assembly of BK and N-type Ca^{2+} channels. Western immunoblots of proteins isolated from soluble whole brain (A,C) or hippocampal (B) extracts by immunoprecipitation using antibodies for the α-subunits of the BK channel (anti-BK$\alpha_{1118\text{-}1135}$; BK-IP) or the $Ca_V2.2$ channel (anti-$Ca_V2.2$; $Ca_V2.2$-IP). (Ai) Probing BK-IP and rabbit IgG IP (IgG-IP) samples with anti-$Ca_V2.2$ revealed a band of ~210 kDa in the BK-IP sample lane but not in the IgG control co-IP lane, indicative of the lower molecular mass form of the $Ca_V2.2$-subunit (n=4). (Aii) Enrichment of the immunoreactive band for the BK channel α-subunit (120 kDa) in the BK-IP sample demonstrated the specificity of the immunoprecipitation. (B) The $Ca_V2.2$-subunit was co-immunoprecipitated with the BK channel α-subunit from solubilised rat hippocampal tissue. This was seen as a band of ~210 kDa in the BK-IP sample, which was absent in the control IgG-IP lane. (Ci) Probing $Ca_V2.2$-IP and rabbit IgG co-IP (IgG-IP) samples with anti-BK produced an immunoreactive band of the predicted molecular mass of BK channel α-subunit (not observed in the IgG control co-IP lane), showing that the BK channel α-subunit reciprocally co-immunoprecipitated with the $Ca_V2.2$-subunit (n=3). (Cii) Enrichment of the immunoreactive band for the $Ca_V2.2$-subunit (210 kDa) in the $Ca_V2.2$-IP sample demonstrated the specificity of the immunoprecipitation. In each of the above, a solubilised whole brain extract (input) was run alongside the co-immunoprecipitation samples. Input was ~5% of total protein extract used in the assay. The positions of channel proteins and the heavy chain IgG (HC IgG) of the immunoprecipitating antibodies are indicated by arrows, and molecular mass standards are shown in each immunoblot.

Cell-attached patches from cells co-expressing the $rSlo_{27}$ and $Ca_V2.2/Ca_V\beta_3$ subunits exhibited inward channel openings (derived from $Ca_V2.2/Ca_V\beta_3$) near coincident with outward channel openings (derived from $rSlo_{27}$) (14 patches exhibited coupled channels, four other patches displayed only rare $rSlo_{27}$ channel openings and three patches showed only $Ca_V2.2/Ca_V\beta_3$ channel activity) (Fig. 3Ci). The very close temporal association was seen as an immediate activation of the $rSlo_{27}$ channel following the opening of the $Ca_V2.2/Ca_V\beta_3$ channel (Fig. 3Cii). Opening of outward channels was observed only with Ca^{2+} as the charge carrier and were not observed in patches where Ba^{2+} (110 mM) was used (n=7, data not shown). Patches displayed single level inward channel activity and a maximum of five outward channels (observed as channel superimpositions evoked by a step to +200 mV, data not shown), indicating that patches exhibited a low number of both channels and that near coincident opening did not result from unduly high expression levels. BK ($rSlo_{27}$) channel openings preceded by an opening of a $Ca_V2.2/Ca_V\beta_3$ (coupled) channel comprised 59% of all BK channel openings observed (85 openings of coupled BK channels from a total of 144 BK channel openings, n=14 patches containing coupled channel openings). The predicted close spatial association of expressed channels was tested by determination of whether intracellular BAPTA could disrupt the functional coupling of $Ca_V2.2/Ca_V\beta_3$ and $rSlo_{27}$ channels. $Ca_V2.2/Ca_V\beta_3$ channel open times were longer from BAPTA-AM treated cells compared with control cells, with the open

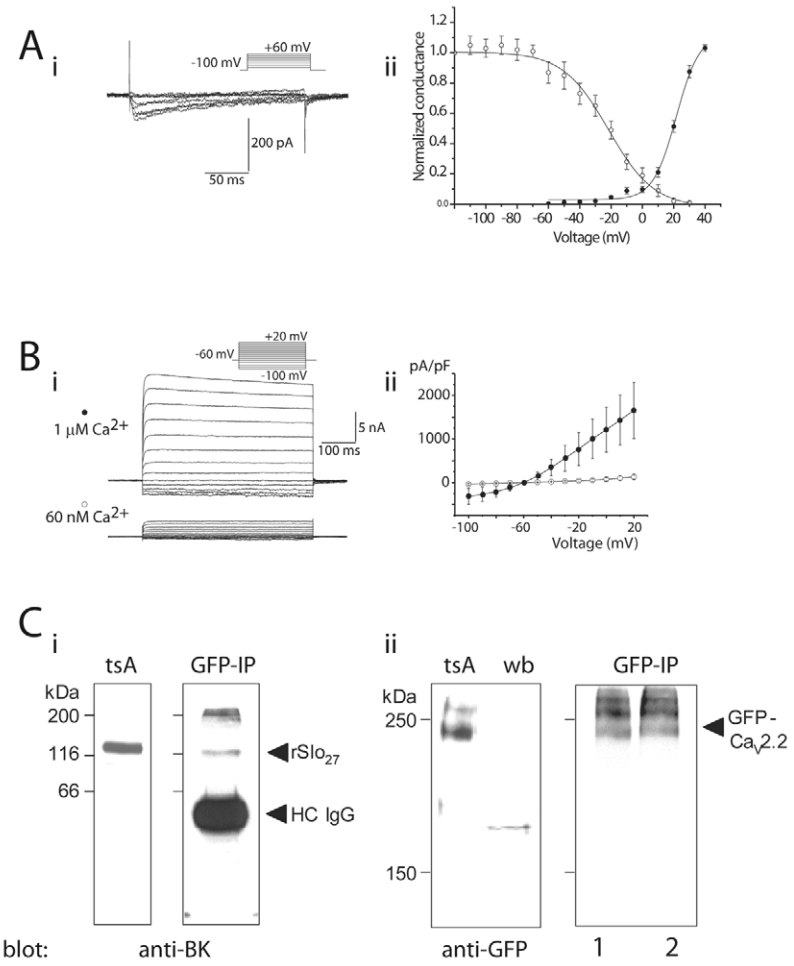

Fig. 2. Expression of only pore-forming α-subunits produced functional current. (Ai) Family of whole-cell currents from a cell transfected with GFP-$Ca_V2.2$ evoked by step depolarisations (–60 to +60 mV) from a holding potential of –100 mV. (Aii) Normalised activation curve (●) was fit by a Boltzmann distribution with a V½ of +21 mV and a slope of e-fold in 7.8 mV (n=12). By contrast, steady-state inactivation was determined by (prepulse) voltage steps (1-second duration) preceding a test pulse (+30 mV) (n=10). The relationship (○) was fit by a Boltzmann distribution of V½ –21 mV. (Bi) Representative macroscopic current sweeps from two cells expressing $rSlo_{27}$, one dialysed with an electrode solution containing 1 μM free Ca^{2+} (upper) and another dialysed with a solution containing 60 nM free Ca^{2+} (lower). (Bii) Mean normalised current-voltage relationship for cells dialysed with either 1 μM (●, n=5) or 60 nM (○, n=5) free Ca^{2+}. (Ci) Expression of $rSlo_{27}$ channels was confirmed by western immunoblotting with anti-BK (tsA). Probing the GFP-IP sample from cells co-transfected with $rSlo_{27}$ and GFP-$Ca_V2.2$ subunits with anti-BK produced a band of ~120 kDa, the predicted molecular mass of the $rSlo_{27}$ channel α-subunit. (Cii) Expression of the GFP-$Ca_V2.2$ subunit in tsA-201 cell lysates (tsA) was confirmed by western immunoblotting using anti-GFP, with anti-GFP immunoreactivity being absent in the rat whole brain (wb) tissue lane. Immunoreactive bands of ~240 and 270 kDa, the predicted molecular masses of the GFP-$Ca_V2.2$ channel protein, were detected in the GFP-IP by both anti-$Ca_V2.2$ (lane 1) and anti-GFP (lane 2).

duration distribution at +20 mV being best fit by a bi-exponential function of time constants 1.4 and 2.7 mseconds. This was in contrast to the monoexponential fit required for $Ca_V2.2/Ca_V\beta_3$ channels under control conditions. In addition, coupled $rSlo_{27}$ channel open times (at +20 mV) were shorter [mean open time reduced from 5.5±0.83 mseconds (control, n=14 patches) to 1.1±0.17 mseconds (BAPTA-AM-treated cells, n=13 patches, P<0.05)] in cells pre-treated with BAPTA-AM. The effects on both inward and outward channel open times showed that pre-treatment of cells with BAPTA-AM caused the intracellular accumulation of BAPTA. Cell-attached patches still exhibited near coincident openings of inward $Ca_V2.2/Ca_V\beta_3$ channels and outward $rSlo_{27}$ channels (Fig. 3Di,ii) (13 patches exhibited coupled channels, 3 patches displayed $rSlo_{27}$ channel openings and 3 patches showed only $Ca_V2.2/Ca_V\beta_3$ channel activity). Coupled BK channel openings comprised 63% of all BK channel activity observed (184 openings of coupled BK channels from a total of 289 BK channel openings, n=13 patches containing coupled channel openings). This suggests that a distance shorter than the buffering length constant for BAPTA (~30 nm) (Naraghi and Neher, 1997) separated $Ca_V2.2/Ca_V\beta_3$ and $rSlo_{27}$ channels. These data are in accord with the functional coupling of N-type Ca^{2+} and BK channels in hippocampal neurons (Marrion and Tavalin, 1998) and supports the proposal that this rapid coupling arises from interaction between channel subunits.

Association of L-type Ca^{2+} channels and BK channels

Ca^{2+} entry through both L- and N-type Ca^{2+} channels activates BK channels in neocortical neurons (Sun et al., 2003) and association between L-type Ca^{2+} and BK channels has been observed in rat whole brain (Grunnet and Kaufmann, 2004; Berkefeld et al., 2006). Immunoblotting an anti-$BK\alpha_{1118\text{-}1135}$ co-IP (BK-IP) sample from rat brain with an antibody directed against the L-type Ca^{2+} channel (anti-$Ca_V1.2$) revealed an immunoreactive band of the predicted molecular mass of the native $Ca_V1.2$ subunit (210 kDa). Enrichment of $Ca_V1.2$ immunoreactivity in the BK-IP confirmed the specificity of the immunoprecipitation. The specificity of interaction was further confirmed by the presence of only a very faint band corresponding to the $Ca_V1.2$ subunit in the control rabbit IgG co-IP (IgG-IP) (Fig. 4A). Densitometric comparison of this data with the co-IP of N-type Ca^{2+} channels by the same antibody (Fig. 1Ai) showed that $Ca_V1.2$ immunoreactivity was 45% weaker than $Ca_V2.2$ immunoreactivity. This weak interaction between L-type Ca^{2+} and BK channels was reminiscent of the co-IP data reported by Grunnet and Kaufmann (Grunnet and Kaufmann, 2004). Thus, the data clearly indicated that the two channel subunits could associate in rat brain, but the association was more prevalent between N-type Ca^{2+} and BK channels.

Cell-attached patches recording from cells co-expressing the $rSlo_{27}$ and $Ca_V1.2/Ca_V\beta_3$ subunits exhibited very rare examples

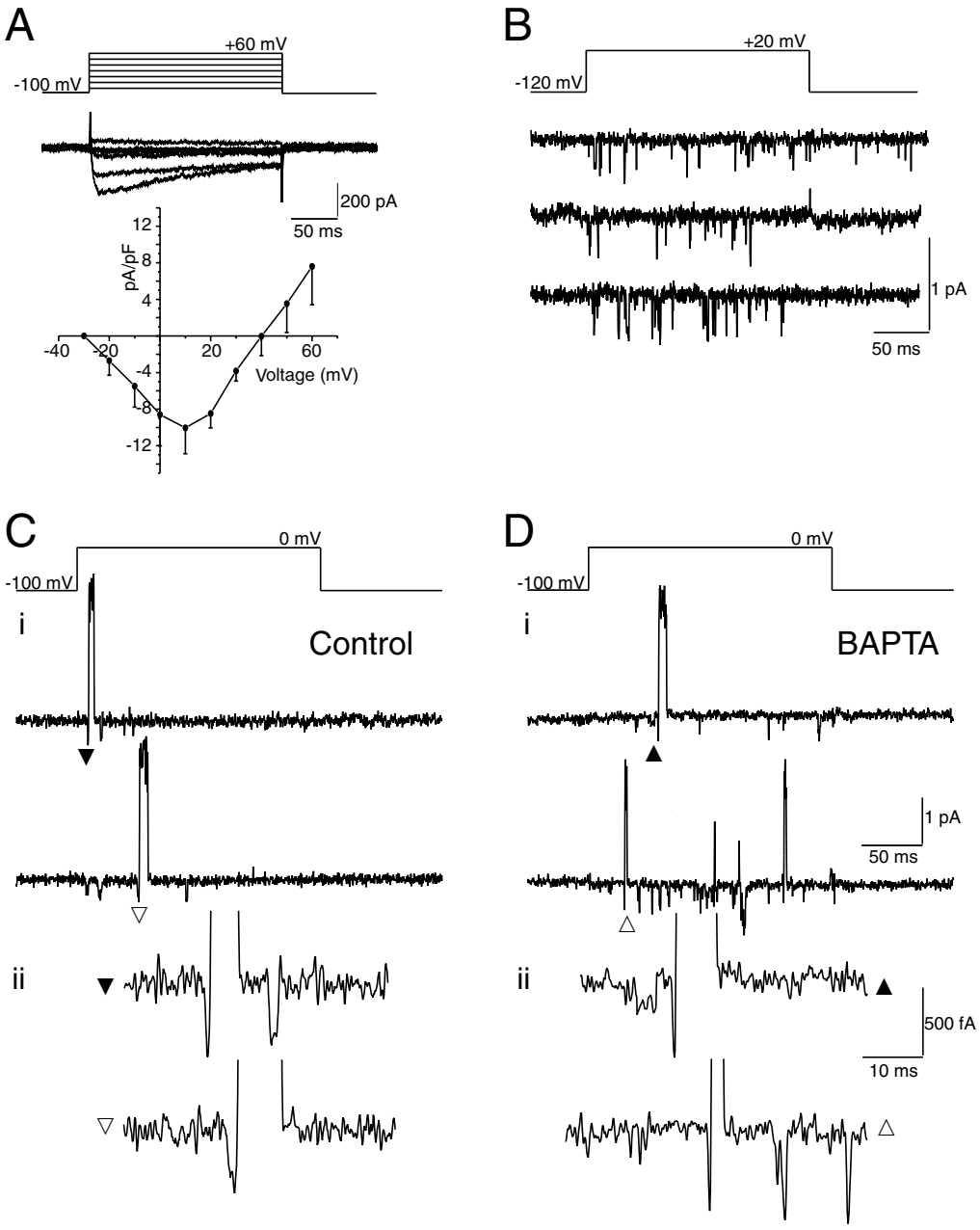

Fig. 3. Functional coupling of N-type Ca^{2+} channels with BK channels reconstituted in tsA-201 cells. (A) Representative macroscopic currents from a cell transfected with GFP-$Ca_V2.2/Ca_V\beta_3$ subunits, evoked from a holding potential of –100 mV by step depolarisations (shown are 20 mV increments) from –60 mV. Below is the normalised current-voltage relationship (n=5). (B) Single channel activity conducted by 160 mM Ca^{2+} evoked by step depolarisations to +20 mV from a holding potential of –120 mV. (Ci) Cell-attached patch records from a cell co-transfected with $rSlo_{27}$ and GFP-$Ca_V2.2/Ca_V\beta_3$ subunits showing near coincident opening of $rSlo_{27}$ channels with inward opening of GFP-$Ca_V2.2/Ca_V\beta_3$ Ca^{2+} channels. The close temporal association of these two expressed channels is seen in the expanded trace (Cii), where the full amplitude of the $rSlo_{27}$ openings has been truncated to resolve coincident openings. (Di) Intracellular BAPTA did not disrupt the coupling between expressed GFP-$Ca_V2.2/Ca_V\beta_3$ and $rSlo_{27}$ channels. Cell-attached patch current sweeps from a BAPTA-AM (10 μM)-treated cell displayed near coincident activation of $rSlo_{27}$ channels following the opening of GFP-$Ca_V2.2/Ca_V\beta_3$ channels. The close temporal coupling of expressed channels is seen in the expanded trace (Dii).

of near coincident inward and outward channel openings (Fig. 4B,C). Inward channel openings (derived from $Ca_V1.2/Ca_V\beta_3$) were of very small amplitude and were observed to both precede and follow outward channel openings (derived from $rSlo_{27}$) (Fig. 4B,C). Fig. 4B,C are examples of data from two different patches, where in one sweep from each patch there was a near coincident opening of inward and outward channels observed. 8 patches displayed inward channel openings (derived from $Ca_V1.2/Ca_V\beta_3$) near coincident with outward channel openings (derived from $rSlo_{27}$) out of 19 patches that contained both channel types (Fig. 4B) (14 other patches displayed only rare $rSlo_{27}$ channel openings and 3 patches showed only $Ca_V1.2/Ca_V\beta_3$ channel activity), but the number of examples of coupled events was extremely small. Rare examples of the functional coupling between $rSlo_{27}$ and $Ca_V1.2/Ca_V\beta_3$ channels subunits gave only 0.4% of $rSlo_{27}$ channel openings that were immediately preceded by an opening of a $Ca_V1.2/Ca_V\beta_3$ (coupled) channel (12 openings of coupled BK channels from a total of 3261 BK channel openings, n=8 patches containing coupled channel openings) (Fig. 4B). This contrasted with 59% of $rSlo_{27}$ channel openings being preceded by an opening of a $Ca_V2.2/Ca_V\beta_3$ (coupled) channel (see above). The observed dearth of coupled channels was consistent with the weak interaction identified by co-IP of channel subunits from rat brain (Fig. 4A).

Functional interplay between N-type Ca^{2+} channels and BK channels during action potential repolarisation in hippocampal CA1 neurons

The effects of the N-type Ca^{2+} channel blocker ω-conotoxin GVIA on action potential (spike) duration was assessed in hippocampal slices to determine whether functional coupling

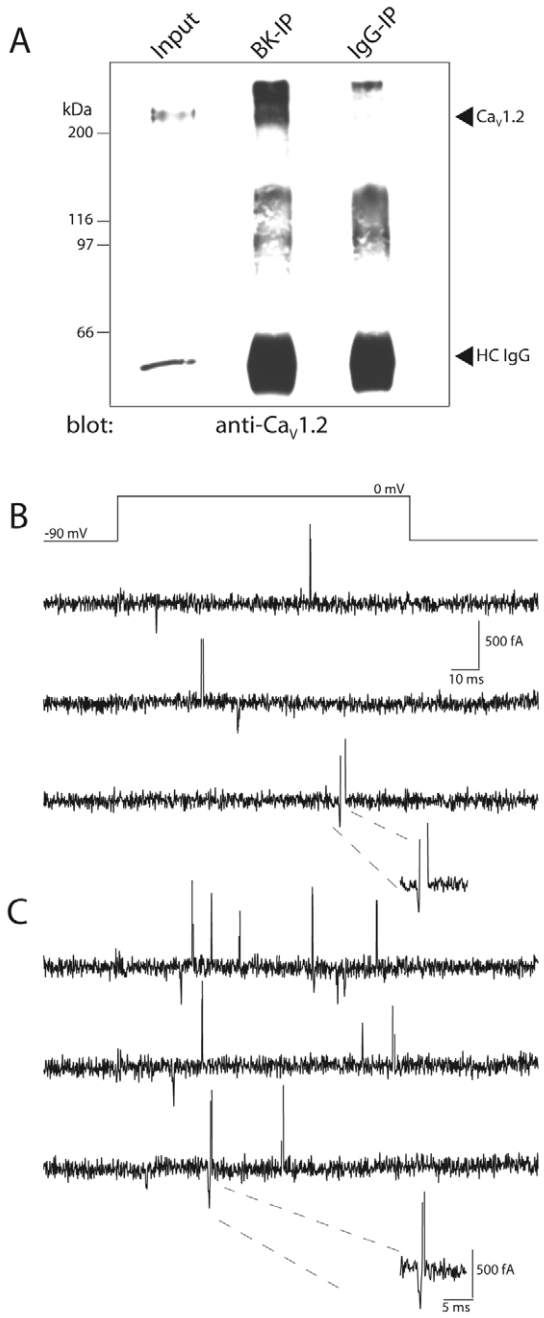

Fig. 4. Association of L-type Ca^{2+} and BK channels. (A) Western immunoblots of proteins isolated from soluble whole brain extracts by immunoprecipitation using anti-BK$\alpha_{1118\text{-}1135}$ (BK-IP). Probing BK-IP and rabbit IgG co-IPs (IgG-IP) samples with anti-$Ca_V1.2$ revealed a weak band of ~210 kDa in the BK-IP sample lane, with a weaker reactivity observed in the IgG control co-IP lane. Enrichment of the immunoreactive band for $Ca_V1.2$ in the BK-IP sample demonstrated the specificity of the immunoprecipitation (n=3). (B,C) Cell-attached patch records from two separate cells co-transfected with $rSlo_{27}$ and $Ca_V1.2/Ca_V\beta_3$ subunits. The vast majority of outward channel openings (derived from $rSlo_{27}$) were not associated with any inward channel opening (derived from $Ca_V1.2/Ca_V\beta_3$). In very rare examples, a near coincident opening of $rSlo_{27}$ channels with inward opening of $Ca_V1.2/Ca_V\beta_3$ Ca^{2+} channels was observed. The close temporal association of these two expressed channels is seen in the expanded trace. The full amplitude of the $rSlo_{27}$ openings has been truncated to resolve the small amplitude inward channel openings.

underlies the physiological activation of BK channels. Evoked spikes were of short duration and exhibited an obvious fast afterhyperpolarisation (fAHP) (Fig. 5Ai, asterisk in inset). Under control conditions, an increase in action potential duration was observed between the first and subsequent spikes within the train, with the broadening of the second spike relative to the first spike being 23.5±1.3% (n=5 cells; 10 spikes per cell, P<0.05). This degree of spike broadening was sustained throughout the train (Fig. 5Aii,iv, open bars). BK channel inactivation (Hicks and Marrion, 1998) has been proposed to contribute to this spike broadening during repetitive firing (Faber and Sah, 2003; Shao et al., 1999). Block of BK channels by iberiotoxin (IbTx, 100 nM) (Fig. 5Ai) or charybdotoxin (ChTx, 10 nM) (Fig. 5Aiii) caused a marked broadening of the lower half of the spike and a concomitant reduction in the fAHP, confirming that BK channel activation hastened action potential repolarisation. The spike broadening caused by either BK channel blocker was sustained throughout the spike train but was contributed less in later spikes by a toxin-sensitive component. Ibtx (100nM) produced significant broadening of the first (24.1±1.7%, P<0.05), second (14.7±1.5%, P<0.05), third (15.6±0.6%, P<0.05) and fourth spikes (17.4±0.9%, P<0.05; n=6, 10 spikes per cell). ChTx (10 nM) also slowed significantly the first (14.2±1.2%, P<0.05), second (7.2±0.6%, P<0.05), third (7.2±0.9%, P<0.05) and fourth spikes (8.1±0.8%, P<0.05; n=3, 10 spikes per cell). This also showed that spike broadening resulting from BK channel inactivation was seen primarily in the second spike, after which inactivated BK channels did not further contribute to spike repolarisation.

Block of N-type Ca^{2+} channels by ω-conotoxin GVIA (300 nM) caused a broadening of the lower half of the action potential and a block of the fAHP (Fig. 5Bi), similar to that seen with either BK channel blocker (Fig. 5A). The ω-conotoxin GVIA-induced broadening was sustained throughout the spike train but was contributed less in later spikes by the toxin-sensitive component (first, 18.2±0.9%, P<0.05; second, 10.7±1.1%, P<0.05; third, 11.2±0.9%, P<0.05; fourth spike, 10.9±0.8%, P<0.05; n=7; 10 spikes per cell; Fig. 5Bii). The effect of ω-conotoxin GVIA was concentration dependent, with 1 μM of the toxin producing a significant broadening of first (45.0±2.3%, P<0.05), second (37.8±1.9%, P<0.05), third (38.2±1.5%, P<0.05) and fourth spikes (37.4±2.0%, P<0.05; n=5; 10 spikes per cell; data not shown). These data show that the effect of ω-conotoxin GVIA was most prominent in the first one or two spikes of the train, when spike broadening owing to BK channel inactivation was less significant.

The role of L-type Ca^{2+} channels coupling to BK channel activation was assessed, because it has been previously reported that L-type Ca^{2+} and BK channels were biochemically associated in rat brain (Fig. 4) (Grunnet and Kaufmann, 2004; Berkefeld et al., 2006). Application of the dihydropyridine (DHP) antagonist isradipine (10 μM) had no effect on spike duration throughout the train (Fig. 5Ci,ii, Fig. 6A,B; n=9; P>0.1). The lack of effect was not the result of access problems, because lower concentrations of isradipine significantly reduced the slow AHP (data not shown) and the Ca^{2+} current recorded in these neurons (Fig. 5B,C inset). In addition, a prolongation of the spike duration was observed when IbTx was applied subsequently in the presence of isradipine (Fig. 6Aii). Specificity

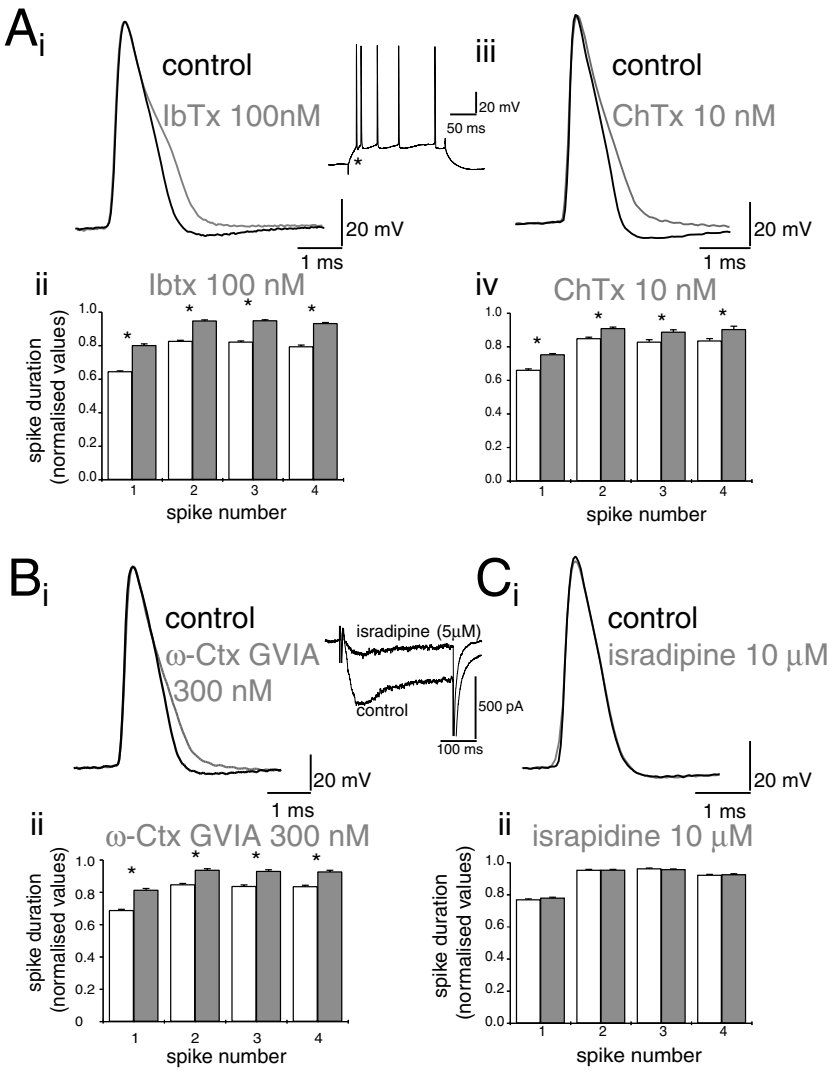

Fig. 5. Selective block of N-type Ca^{2+} channels prolonged action potential duration. (Ai) Example action potentials showing action potential broadening and block of the fast afterhyperpolarisation (fAHP) by application of the BK channel blocker iberiotoxin (IbTx, 100 nM). All spike traces refer to the first spike of the train. Inset shows an action potential train of five spikes in a CA1 pyramidal neuron from a hippocampal slice evoked by a 200 msecond depolarising current injection. * indicates the fAHP. (Aii) Normalised pooled data showing the slowing of action potential duration during a train of action potentials resulting from BK channel inactivation (open bars, see text). Shaded bars show that the slowing of action potential duration by IbTx (100 nM) is observed throughout the train, with the effect being sustained after the second action potential (n=6 cells, 10 spikes per cell, this and subsequent pooled data plots; *P<0.05). (Aiii) Example action potentials illustrating the slowing of action potential repolarisation and block of the fAHP after addition of the BK channel blocker charybdotoxin (ChTx, 10 nM). (Aiv) Normalised pooled data showing that the prolongation of action potential duration by ChTx was sustained throughout the train (n=3 cells, 10 spikes per cell). (Bi) Block of N-type Ca^{2+} channels by ω-conotoxin GVIA (ω-Ctx GVIA, 300 nM) slowed the lower half of action potential repolarisation and abolished the fAHP. (Bii) The normalised pooled data showed that ω-Conotoxin GVIA (300 nM) significantly slowed spike repolarisation of the first and subsequent spikes in a train (n=7 cells, 10 spikes per cell). Inset shows P/4 leak-subtracted whole-cell currents evoked by a 300 msecond depolarising voltage step to 0 mV from a holding potential of –70 mV. Evoked current was greatly reduced by application of isradipine (5 μM), indicating that L-type Ca^{2+} channels carried the majority of inward current. (Ci) Example action potentials showing that selective block of L-type Ca^{2+} channels by the dihydropyridine antagonist isradipine (10 μM) had no effect on action potential duration. (Cii) The lack of an effect for all action potentials within the train is shown in the normalised pooled data (n=9 cells, 10 spikes per cell).

of coupling was demonstrated when isradipine (10 μM) failed to affect spike duration, but subsequent application of ω-Ctx GVIA (300 nM) in the continued presence of the DHP antagonist broadened spike duration as seen before (Fig. 6Bi,ii). Finally, application of ω-Ctx GVIA (300 nM) had no effect when it was applied after BK channels had been blocked by prior application of IbTx (Fig. 6Ci,ii). These data confirmed that the effect of N-type Ca^{2+}-channel block was not additive to direct the block of BK channels by IbTx. This demonstrated that block of N-type Ca^{2+} channels by ω-conotoxin GVIA caused spike broadening by preventing BK channel activation during the falling phase of the action potential. In addition, these data show that action potential repolarisation is primarily hastened by activation of coupled BK channels. The results demonstrated that specific functional coupling underlies rapid activation of BK channels to hasten spike repolarisation in hippocampal neurons.

Discussion

Both N-type Ca^{2+} and BK channels have been shown to be associated with different proteins. Apart from the auxillary β- and $\alpha_2\delta$-subunits, the pore-forming subunit for N-type channels ($Ca_V2.2$) is known to associate with syntaxin (Sheng et al., 1994), Ras (Richman et al., 2004), G protein βγ subunits (Zamponi et al., 1997) and calmodulin (Liang et al., 2003). By contrast, mammalian BK channels associate with syntaxin (Cibulsky et al., 2005; Ling et al., 2003) and the β_2-adrenergic receptor (Liu et al., 2004). The reported interaction of mSlo BK channels with syntaxin excluded the interaction between syntaxin and $Ca_V2.2$ (Cibulsky et al., 2005). Lack of endogenous syntaxin in tsA-201 cells (data not shown) and previous work (Leveque et al., 1994) suggests that a common association with syntaxin did not mediate the association of $rSlo_{27}$ and $Ca_V2.2$ subunits.

The use of pharmacological inhibition to identify coupling between Ca^{2+} and Ca^{2+}-activated channels cannot distinguish between discrete channel co-localisation and a looser association where channels share a common subcellular localisation. Our data demonstrated an association between N-type and BK channel α-subunits in rat brain, which was reconstituted when only the α-subunits were expressed in a

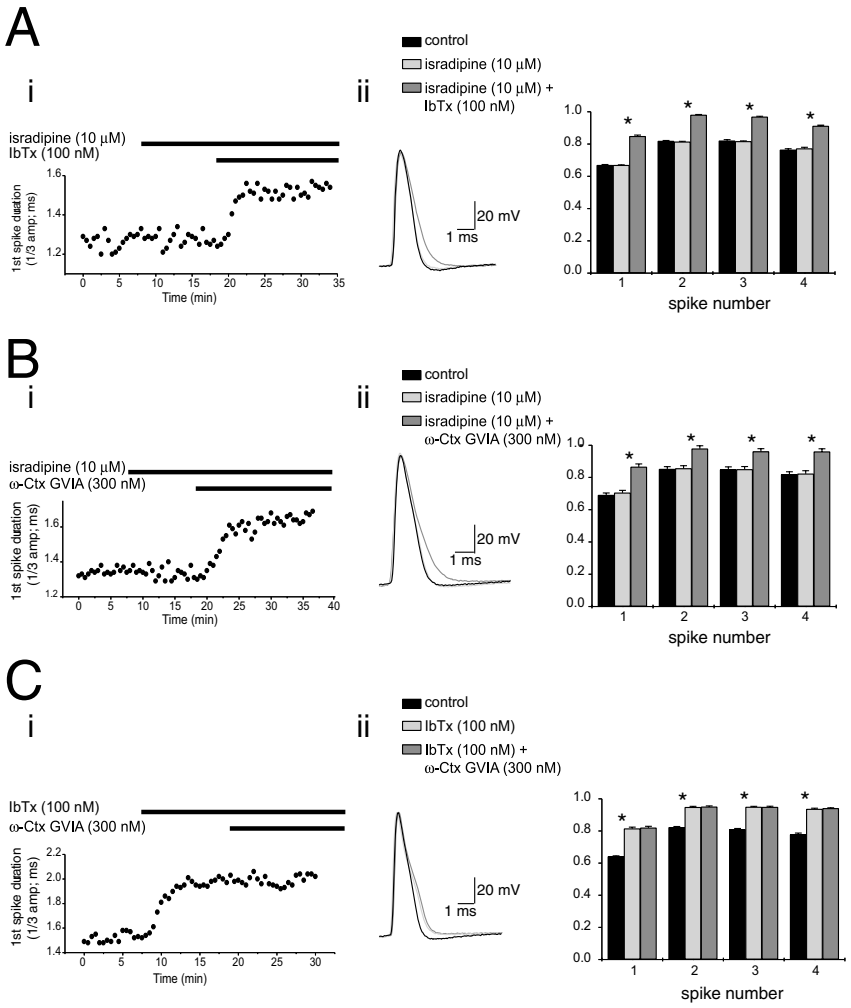

Fig. 6. Cumulative addition of channel blockers demonstrates selective coupling of N-type Ca^{2+} and BK channels. (Ai) Diary plot of the duration of the first action potential in the evoked train from a single hippocampal neuron recorded in a slice preparation. Application of the L-type Ca^{2+} channel dihydropyridine antagonist isradipine (10 μM) had no effect on action potential duration. By contrast, subsequent application of the BK channel blocker iberiotoxin (IbTx, 100 nM) in the presence of the DHP antagonist slowed action potential repolarisation. (Aii) Examples of action potentials taken from the cell used in Ai, recorded before (control) and after addition of isradipine (10 μM) and isradipine (10 μM) + IbTx (100 nM). A clear prolongation of action potential duration is seen after IbTx addition (superimposed traces in black, control; light grey, isradipine; dark grey, isradipine+IbTx). In addition, a bar chart is shown of normalised action potential duration showing the broadening of action potentials during a train in the absence and presence of channel blockers. No effect of isradipine (10 μM) is seen, while further concomitant addition of IbTx (100 nM) slowed action potential repolarisation throughout the train (*n*=3, 10 spikes per cell). (Bi) Diary plot of duration of the first action potential in the evoked train showing that isradipine (10 μM) had no effect. In contrast, addition of the N-type Ca^{2+} channel blocker ω-conotoxin GVIA (ω-Ctx GVIA, 300 nM) slowed action potential repolarisation. (Bii) Example action potentials from the experiment shown in Bi, showing the action potential broadening only after application of ω-Ctx GVIA (300 nM). Normalised pooled data showed that the effect of ω-Ctx GVIA was observed throughout the train of action potentials (*n*=5 cells, 10 spikes per cell). (Ci) Diary plot of action potential duration showing that ω-Ctx GVIA (300 nM) had no effect if BK channels were pre-blocked by IbTx (100 nM). (Cii) Example action potentials from the experiment illustrated in Ci, showing action potential duration was prolonged by IbTx (100 nM) with no further effect of ω-Ctx GVIA (300 nM). The normalised pooled data showed that the effect of IbTx was observed throughout the train of action potentials, with no effect of subsequent addition of ω-Ctx GVIA (*n*=4, 10 spikes per cell).

non-neuronal cell line. Expression of both α-subunits (plus $Ca_V\beta_3$) in tsA-201 cells provided functional coupling in cell-attached patches that was identical to that observed in hippocampal CA1 pyramidal neurons (Marrion and Tavalin, 1998). This was in contrast to data obtained from cells expressing L-type ($Ca_V1.2$ plus $Ca_V\beta_3$) and $rSlo_{27}$ subunits, where only extremely rare examples of coupled openings were observed. This paucity of functional coupling was consistent with the weaker association of the two channel subtypes in brain and the lack of coupling between native L-type and BK channels in hippocampal neurons (Marrion and Tavalin, 1998). The use of intracellular Ca^{2+} buffers, such as EGTA and BAPTA can provide invaluable information regarding the relative location of Ca^{2+} and Ca^{2+}-activated channels. For example, activation of BK channels in chromaffin cells required Ca^{2+} entry through both L-type and Q-type channels (Prakriya and Lingle, 1999). Most BK channels were found to be close enough to Ca^{2+} channels to be resistant to high concentrations of EGTA, but activation was blocked by BAPTA (Prakriya and Lingle, 2000; Berkefeld et al., 2006). These data suggested that some distance [estimated to be between 50 and 160 nm by Prakriya and Lingle (Prakriya and Lingle, 2000)] between Ca^{2+} and BK channels exists in this cell type. This distance was proposed to separate L-type Ca^{2+} and SK channels in hippocampal neurons, partly because this coupling was sensitive to intracellular BAPTA (Marrion and Tavalin, 1998). By contrast, the rapid coupling observed between N-type and BK channels in this study and in the hippocampus was insensitive to BAPTA. Our data have demonstrated that the channel α-subunits are very close and it is possible that the interaction is direct. The interaction occurred when only the α-subunits were expressed in a non-neuronal cell-line. This was complicated by the inability to resolve single $Ca_V2.2$ channel openings when expressed alone, requiring co-expression of $Ca_V\beta_3$ subunits to enable recording of single channel activity. The observed functional coupling could have resulted from association between $Ca_V\beta_3$ and Slo_{27} subunits. This is unlikely to be the case, because co-expression of $Ca_V1.2/Ca_V\beta_3$ and $rSlo_{27}$ channels gave only

very rare examples of rapid functional coupling. These data suggested that it is probable that the association between $Ca_V2.2$ and $rSlo_{27}$ channels was direct between the pore-forming subunits, but if the interaction was mediated by an intermediate protein it would have to be common to both tsA-201 cells and hippocampal neurons.

This is the first study to show that association between α-subunits underlies rapid functional coupling between Ca^{2+} and Ca^{2+}-activated channels. This type of association is best suited to the activation of BK channels, because of their requirement for high micromolar Ca^{2+} concentrations (Vergara et al., 1998). A direct association of the N-type Ca^{2+} and BK channel is particularly well suited to provide the rapid activation of BK channels that is required to hasten action potential repolarisation. Recorded action potentials had a duration of approximately 1.2 mseconds (Figs 5 and 6). N-type Ca^{2+} channels only open during the second half of the falling phase of the spike (Helton et al., 2005). For a selective functional coupling between N-type Ca^{2+} and BK channels to achieve spike brevity, it is necessary that N-type Ca^{2+} channels open, Ca^{2+} ions enter the cell and BK channels are activated in less than a few hundred microseconds. We have observed that there was an almost instantaneous activation of $rSlo_{27}$ channels upon the opening of a functionally coupled $Ca_V2.2$ channel. This behaviour was identical to that seen with native N-type Ca^{2+} and BK channels in hippocampal neurons (Marrion and Tavalin, 1998). These data were consistent with the biochemical data showing association of pore-forming α-subunits. All these data clearly indicate that selective co-assembly is required for BK channels to play their role in hastening action potential repolarisation.

This study has confirmed the physiological relevance of association between α-subunits of N-type Ca^{2+} and BK channels. The hastening of action potential repolarisation in hippocampal neurons results from activation of BK channels by Ca^{2+} entry through colocalised N-type Ca^{2+} channels, showing that functional coupling between specific channel subtypes is used to maintain spike brevity. The lack of an effect on action potential duration of the L-type Ca^{2+} channel blocker isradipine appeared to contrast with the biochemical data reporting an association between L-type Ca^{2+} and BK channels in brain (Grunnet and Kaufmann, 2004; Berkefeld et al., 2006). However, we showed that association of L-type and BK channels in brain was much weaker than that seen with N-type and BK channels: an association that was mirrored in co-IP data reported by Grunnet and Kaufmann (Grunnet and Kaufmann, 2004). It is likely that association between L-type Ca^{2+} and BK channels may underlie the activation of BK channels in other CNS neurons (Sun et al., 2003). The finding that mainly N-type channels provide the Ca^{2+} entry for activation of BK channels is in accord with both channel subtypes displaying a common subcellular location (Sausbier et al., 2006; Westenbroek et al., 1992), while L-type and BK channels are not necessarily in the same subcellular compartment in CNS neurons (Hell et al., 1993; Bowden et al., 2001; Sausbier et al., 2006). Application of ω-conotoxin GVIA to hippocampal neurons had no significant effect on spike firing patterns and adaptation during a burst, which are regulated by other Ca^{2+}-activated potassium conductances [medium and slow AHPs (data not shown) (Lancaster and Nicoll, 1987; Vergara et al., 1998)]. This supports cell-attached patch data from hippocampal neurons (Marrion and Tavalin, 1998) showing that the functional coupling between N-type Ca^{2+} and BK channels is selective.

Materials and Methods

Solubilisation of rat brain membranes

Brains or dissected hippocampi from 9-12 day old Wistar rats were homogenised in ice-cold buffer (10 mM HEPES, 350 mM sucrose, 5 mM EDTA, pH 7.4) and centrifuged (2000 ***g***) at 4°C for 5 minutes. All buffers contained the protease inhibitors: pepstatin A (1 μg/ml), leupeptin (1 μg/ml), aprotinin (1 μg/ml), Pefabloc SC (0.2 mM), benzamidine (0.1 mg/ml) and calpain inhibitors I and II (8 μg/ml each). The supernatant was centrifuged (100,000 ***g***) at 4°C for 1 hour and the membrane pellet resuspended in ice-cold buffer (2 mg/ml). Membrane proteins were solubilised (10 mM HEPES, 5 mM EDTA, pH 7.4 containing 1.2% digitonin) at 4°C for 1 hour and insoluble material removed by centrifugation (100,000 ***g***) at 4°C for 1 hour.

Co-immunoprecipitation (co-IP) from rat brain

Solubilised rat brain lysates (~1.0-2.0 mg/ml) were incubated with protein A-Sepharose (BK channel co-IPs) or protein A/G agarose (N-type Ca^{2+} channel/$Ca_V2.2$ co-IPs) for 3 hours at 4°C to remove non-specific interactions. Precleared solubilised proteins were incubated with either rabbit polyclonal anti-$BK\alpha_{1118\text{-}1135}$ (Wanner et al., 1999) or rabbit polyclonal anti-$Ca_V2.2$ (Chemicon International, CA) for 12-15 hours at 4°C. Protein A-Sepharose or protein A/G agarose was added and the mixture incubated at 4°C for 3 hours to capture immunoprecipitated proteins. The beads were washed with buffer (10 mM HEPES, 150 mM NaCl, 5 mM EDTA, pH 7.4 containing 0.2% digitonin) and bound proteins were eluted with 1× SDS sample buffer, resolved by 6-10% SDS-PAGE and transferred to PVDF membrane. Membranes were blocked with 5% non-fat milk (dissolved in PBS-T: 137 mM NaCl, 2.7 mM KCl, 8.1 mM Na_2HPO_4, 1.5 mM KH_2PO_4, 0.1% Tween-20) for 12-15 hours at 4°C and either incubated with rabbit polyclonal anti-BK (Chemicon International, CA; 1:250), rabbit polyclonal anti-$Ca_V2.2$ (Chemicon International; 1:150) or rabbit polyclonal anti-$Ca_V1.2$ (Alomone Laboratories, Jerusalem, Israel; 1:250). Immunolabelled bands were resolved using a rabbit IgG HRP-conjugated secondary antibody and visualised using ECL (Amersham Pharmacia, UK). Enrichment of protein in the immunoprecipitation was used to confirm the specificity of the immunoprecipitating antibody, with enrichment being observed when a solubilised whole brain extract (input) was run alongside the co-immunoprecipitation samples. Input was ~5% of total protein extract used in the assay.

Co-immunoprecipitation from tsA-201 cells

Cells were transfected using Superfect™ (Qiagen, UK) with plasmids encoding the α-subunits GFP-$Ca_V2.2$ (Raghib et al., 2001) and $rSlo_{27}$, a variant of the BK channel α-subunit that is highly expressed in the hippocampus (Ha et al., 2000), at a 1:1 plasmid DNA ratio. Cells were harvested after 24-36 hours in lysis buffer (25 mM Tris-HCl, 250 mM NaCl, 5 mM EDTA, pH 7.5 containing 1% digitonin), incubated at 4°C for 1 hour, and insoluble material was removed by centrifugation (12,000 ***g***) at 4°C for 10 minutes. Solubilised cell lysates (~1.0 mg/ml) were incubated with protein A-Sepharose and precleared solubilised proteins were incubated with rabbit polyclonal anti-GFP (Santa Cruz Biotechnology, CA) for 12-15 hours at 4°C. Protein A-Sepharose was added and the mixture incubated at 4°C for 3 hours to capture immunoprecipitated proteins. The beads were washed with lysis buffer and bound proteins were processed as above. Membranes were western immunoblotted with anti-BK to resolve $rSlo_{27}$ expression, and either anti-GFP or anti-$Ca_V2.2$ to resolve GFP-$Ca_V2.2$ expression.

Recording from tsA-201 cells

tsA-201 cells were co-transfected with plasmids encoding GFP-$Ca_V2.2$, $Ca_V1.2$, $CaV\beta_3$, $rSlo_{27}$ and EGFP using 1:1:1:0.1 ratio of plasmids and used after 24-36 hours. For GFP-$Ca_V2.2$, cells were superfused with an external solution of composition: 100 mM TEACl, 2.5 mM KCl, 1 mM $MgCl_2$, 10 mM HEPES, 60 mM $BaCl_2$, pH 7.4. Electrodes were fabricated from KG-33 glass and filled with: 120 mM $CsMeSO_4$, 20 mM TEA, 1.5 mM $MgCl_2$, 15 mM Na_2ATP, 10 mM EGTA, 80 mM free $CaCl_2$, pH 7.4. Whole-cell recordings for GFP-$Ca_V2.2/Ca_V\beta_3$ channels were as above, except extracellular $CaCl_2$ was 5 mM and intracellular EGTA was 0.5 mM. Currents were recorded using an Axopatch 200A with electrode resistances of 2-4 MΩ. Capacitance and series-resistance compensation was used throughout. Currents were evoked by 200-msecond voltage steps (–50 to +30 mV) from a holding potential of –100 mV, low pass filtered at 1 kHz through an eight-pole Bessel filter and acquired at 100 μsecond intervals using PULSE (Heka, Germany). Currents were leak-subtracted using a P/4 protocol. For $rSlo_{27}$, cells were superfused with a solution (*) containing: 144 mM NaCl, 2.5 mM KCl, 1.2 mM $MgCl_2$, 2.5 mM $CaCl_2$, 10 mM HEPES, 5.6 mM D-glucose, pH 7.4. Whole-cell electrodes were filled with (+): 130 mM $KMeSO_4$, 20 mM KCl, 1.5 mM K_2ATP, 10 mM HEPES,

10 mM EGTA, 3 mM $MgCl_2$, 9.62 mM $CaCl_2$ (1 μM free) or 3.62 mM $MgCl_2$, 6.02 mM $CaCl_2$ (60 nM free), pH 7.4.

Inward GFP-$Ca_V2.2$/$Ca_V\beta_3$ channel currents were recorded using quartz electrodes (7-10 MΩ) filled with 160 mM $CaCl_2$ (Marrion and Tavalin, 1998). For $rSlo_{27}$, excised inside-out patch recordings were made using quartz electrodes filled with the solution * described above and bathed in solution +, with $rSlo_{27}$ channel activity evoked by raising the bath Ca^{2+} concentration to 1 μM. All single channel currents were filtered at 1 kHz (eight-pole Bessel) and acquired at 100-μsecond intervals. Single channels were analysed with TAC (Bruxton) using the 50% threshold technique. Cell-attached patches from cells co-transfected with $Ca_V2.2$/$Ca_V\beta_3$ or $Ca_V1.2$/$Ca_V\beta_3$ and $rSlo_{27}$ subunits were obtained with the solutions used for resolving $Ca_V2.2$/$Ca_V\beta_3$ channel activity described above, with functional coupling resolved by a step depolarisation from a holding potential of –100 mV ($Ca_V2.2$/$Ca_V\beta_3$) or –90 mV ($Ca_V1.2$/$Ca_V\beta_3$) to 0 mV for 500 mseconds (Marrion and Tavalin, 1998).

Hippocampal slice preparation and recording

Hippocampal slices (350 μm thick) were cut from Wistar rats (20-24 days old) in ice-cold artificial CSF (ACSF), which contained: 125 mM NaCl, 2.5 mM KCl, 25 mM $NaHCO_3$, 16 mM D-glucose, 1.25 mM KH_2PO_4, 1 mM $MgCl_2$ and 1 mM $CaCl_2$, pH 7.4 (bubbled with 95% O_2/5% CO_2). Slices were stored in ACSF at room temperature in a humidified interface chamber for >1 hour and then transferred to the recording chamber mounted on an Axioskop 2 FS (Zeiss, Germany) and continuously superfused at 30°C with ACSF (with $CaCl_2$ raised to 2.5 mM). CA1 pyramidal neurons were visualised using infrared DIC. Whole-cell electrodes (5-9 MΩ) filled with a pipette solution containing: 135 mM potassium-D-gluconate, 10 mM KCl, 10 mM HEPES, 1 mM $MgCl_2$, 2 mM Na_2ATP and 0.4 mM Na_3GTP (280-300 mOsm), pH 7.2-7.3 with KOH. Membrane voltage was recorded using an AxoClamp 2B amplifier (Axon Instruments, CA) in bridge current-clamp mode, low-pass filtered at 3 kHz (eight-pole Bessel, Frequency Devices, CT) and acquired at 20 kHz using PULSE (HEKA, Germany). Only cells with a membrane potential more negative than –60 mV were used, with the membrane potential maintained at –60 mV by injection of depolarising current. Action potentials (5 spikes/pulse) were evoked by depolarising current injection (200 mseconds duration every 30 seconds). Action potential duration was measured at one-third of the total spike amplitude (measured from the threshold level). Analysis of the fifth spike was not included because it occasionally coincided with the end of the current injection. Drug effects on spike duration were assessed by comparing mean action potential duration (obtained from measurement of ten action potentials) before and during application of channel blocker (determined after 10 minutes if no effect was apparent or after the effect had stabilised – see time-courses in Fig. 6). Effect on spike duration was presented, with duration normalised to the longest duration measured in the same experiment. Significance was determined using the student's *t*-test, with values expressed as mean ± s.e.m. Ca^{2+} current measurements were carried out by whole-cell recording using an electrode solution containing: 120 mM $CsMeSO_4$, 30 mM TEA, 10 mM BAPTA, 5 mM $MgCl_2$, 5 mM Na_2ATP, 10 mM HEPES (pH 7.2), with slices bathed in the ACSF detailed above (with extracellular $CaCl_2$ raised to 10 mM). Membrane currents were evoked from a holding potential of –70 mV, filtered at 1 kHz and acquired at 10 kHz.

We thank Hans-Günther Knaus (University of Innsbruck, Austria) for anti-$BK\alpha_{1118-1135}$, Chul-Seung Park (Gwangju Institute of Science and Technology, Korea) for $rSlo_{27}$, Annette Dolphin (UCL, UK) for providing GFP-$Ca_V2.2$, Yoichi Yamada (Sapporo Medical University, Japan) for $Ca_V1.2$ and Kevin Campbell (University of Iowa, USA) for donating $Ca_V\beta_3$. tsA-201 cells were kindly provided by David Brown. We thank Dewi Roberts and Jenna Montgomery for technical assistance. We wish to thank Michael Shipston and Dawn Shepherd for critical reading of the manuscript. This work was supported by the MRC (UK).

References

Alioua, A., Mahajan, A., Nishimaru, K., Zarei, M. M., Stefani, E. and Toro, L. (2002). Coupling of c-Src to large conductance voltage- and Ca^{2+}-activated K^+ channels as a new mechanism of agonist-induced vasoconstriction. *Proc. Natl. Acad. Sci. USA* **99**, 14560-14565.

Berkefeld, H., Sailer, C. A., Bildl, W., Rohde, V., Thumfart, J.-O., Eble, S., Klugbauer, N., Reisinger, E., Bischofberger, J., Oliver, D. et al. (2006). BK_{Ca}-Cav channel complexes mediate rapid and localized Ca^{2+}-activated K^+ signalling. *Science* **314**, 615-620.

Bowden, S. E. H., Fletcher, S., Loane, D. L. and Marrion, N. V. (2001). Somatic co-localization of rat SK1 and D class ($Ca_V1.3$) L-type calcium channels in rat CA1 hippocampal pyramidal neurons. *J. Neurosci.* **21**, 1-6.

Butcher, A. J., Leroy, J., Richards, M. W., Pratt, W. S. and Dolphin, A. C. (2006). The importance of occupancy rather than affinity of $Ca_V\beta$ subunits for the calcium channel I-II linker in relation to calcium channel function. *J. Physiol.* **574**, 387-398.

Cibulsky, S. M., Fei, H. and Levitan, I. B. (2005). Syntaxin-1A binds to and modulates the Slo calcium-activated potassium channel via an interaction that excludes syntaxin binding to calcium channels. *J. Neurophysiol.* **93**, 1393-1405.

Davare, M. A., Dong, F., Rubin, C. S. and Hell, J. W. (1999). The A-kinase anchor protein MAP2B and cAMP-dependent protein kinase are associated with class C L-type calcium channels in neurons. *J. Biol. Chem.* **274**, 30280-30287.

Edgerton, J. R. and Reinhart, P. H. (2003). Distinct contributions of small and large conductance Ca^{2+}-activated K^+ channels to rat Purkinje neuron function. *J. Physiol.* **548**, 53-69.

Faber, E. S. and Sah, P. (2003). Ca^{2+}-activated K^+ (BK) channel inactivation contributes to spike broadening during repetitive firing in the rat lateral amygdala. *J. Physiol.* **552**, 483-497.

Faber, E. S., Delaney, A. J. and Sah, P. (2005). SK channels regulate excitatory synaptic transmission and plasticity in the lateral amygdala. *Nat. Neurosci.* **8**, 635-641.

Grunnet, M. and Kaufmann, W. A. (2004). Coassembly of big conductance Ca^{2+}-activated K^+ channels and L-type voltage-gated Ca^{2+} channels in rat brain. *J. Biol. Chem.* **279**, 36445-36453.

Ha, T. S., Jeong, S. Y., Cho, S. W., Jeon, H., Roh, G. S., Choi, W. S. and Park, C. S. (2000). Functional characteristics of two BKCa channel variants differentially expressed in rat brain tissues. *Eur. J. Biochem.* **267**, 910-918.

Hallworth, N. E., Wilson, C. J. and Bevan, M. D. (2003). Apamin-sensitive small conductance calcium-activated potassium channels, through their selective coupling to voltage-gated calcium channels, are critical determinants of the precision, pace, and pattern of action potential generation in rat subthalamic nucleus neurons in vitro. *J. Neurosci.* **23**, 7525-7542.

Hell, J. W., Westenbroek, R. E., Warner, C., Ahlijanian, M. K., Prystay, W., Gilbert, M. M., Snutch, T. P. and Catterall, W. A. (1993). Identification and differential subcellular localization of the neuronal class C and class D L-type calcium channel alpha 1 subunits. *J. Cell Biol.* **123**, 949-962.

Helton, T. D., Xu, W. and Lipscombe, D. (2005). Neuronal L-type calcium channels open quickly and are inhibited slowly. *J. Neurosci.* **25**, 10247-10251.

Hicks, G. A. and Marrion, N. V. (1998). Ca^{2+}-dependent inactivation of large conductance Ca^{2+}-activated K^+ (BK) channels in rat hippocampal neurones produced by pore block from an associated particle. *J. Physiol.* **508**, 721-734.

Hirschberg, B., Maylie, J., Adelman, J. P. and Marrion, N. V. (1998). Gating of recombinant small-conductance Ca-activated K^+ channels by calcium. *J. Gen. Physiol.* **111**, 565-581.

Isaacson, J. S. and Murphy, G. J. (2001). Glutamate-mediated extrasynaptic inhibition: direct coupling of NMDA receptors to Ca^{2+}-activated K^+ channels. *Neuron* **31**, 1027-1034.

Lancaster, B. and Nicoll, R. A. (1987). Properties of two calcium-activated hyperpolarizations in rat hippocampal neurones. *J. Physiol.* **389**, 187-203.

Leroy, J., Richards, M. S., Butcher, A. J., Nieto-Rostro, M., Pratt, W. S., Davies, A. and Dolphin, A. C. (2005). Interaction via a key tryptophan in the I-II Linker of N-type calcium channels is required for β1 but not for palmitoylated β2, implicating an additional binding site in the regulation of channel voltage-dependent properties. *J. Neurosci.* **25**, 6984-6996.

Leveque, C., el Far, O., Martin-Moutot, N., Sato, K., Kato, R., Takahashi, M. and Seagar, M. J. (1994). Purification of the N-type calcium channel associated with syntaxin and synaptotagmin. A complex implicated in synaptic vesicle exocytosis. *J. Biol. Chem.* **269**, 6306-6312.

Liang, H., DeMaria, C. D., Erickson, M. G., Mori, M. X., Alseikhan, B. A. and Yue, D. T. (2003). Unified mechanisms of Ca^{2+} regulation across the Ca^{2+} channel family. *Neuron* **39**, 951-960.

Ling, S., Woronuk, G., Sy, L., Lev, S. and Braun, A. P. (2000). Enhanced activity of a large conductance, calcium-sensitive K^+ channel in the presence of Src tyrosine kinase. *J. Biol. Chem.* **275**, 30683-30689.

Ling, S., Sheng, J. Z., Braun, J. E. and Braun, A. P. (2003). Syntaxin 1A co-associates with native rat brain and cloned large conductance, calcium-activated potassium channels in situ. *J. Physiol.* **553**, 65-81.

Liu, G., Shi, J., Yang, L., Cao, L., Park, S. M., Cui, J. and Marx, S. O. (2004). Assembly of a Ca^{2+}-dependent BK channel signaling complex by binding to beta2 adrenergic receptor. *EMBO J.* **23**, 2196-2205.

Marrion, N. V. and Tavalin, S. J. (1998). Selective activation of Ca^{2+}-activated K^+ channels by co-localized Ca^{2+} channels in hippocampal neurons. *Nature* **395**, 900-905.

Naraghi, M. and Neher, E. (1997). Linearized buffered Ca^{2+} diffusion in microdomains and its implications for calculation of $[Ca^{2+}]$ at the mouth of a calcium channel. *J. Neurosci.* **17**, 6961-6973.

Prakriya, M. and Lingle, C. J. (1999). BK channel activation by brief depolarizations requires Ca^{2+} influx through L- and Q-type Ca^{2+} channels in rat chromaffin cells. *J. Neurophysiol.* **81**, 2267-2278.

Prakriya, M. and Lingle, C. J. (2000). Activation of BK channels in rat chromaffin cells requires summation of Ca^{2+} influx from multiple Ca^{2+} channels. *J. Neurophysiol.* **84**, 1123-1135.

Raghib, A., Bertaso, F., Davies, A., Page, K. M., Meir, A., Bogdanov, Y. and Dolphin, A. C. (2001). Dominant-negative synthesis suppression of voltage-gated calcium channel Cav2.2 induced by truncated constructs. *J. Neurosci.* **21**, 8495-8504.

Richman, R. W., Tombler, E., Lau, K. K., Anantharam, A., Rodriguez, J., O'Bryan, J. P. and Diverse-Pierluissi, M. A. (2004). N-type Ca^{2+} channels as scaffold proteins in the assembly of signaling molecules for GABAB receptor effects. *J. Biol. Chem.* **279**, 24649-24658.

Sausbier, U., Sausbier, M., Sailer, C. A., Arntz, C., Knaus, H. G., Neuhuber, W. and

Ruth, P. (2006). Ca(2+)-activated K(+) channels of the BK-type in the mouse brain. *Histochem. Cell Biol.* **125**, 725-741.

Shao, L. R., Halvorsrud, R., Borg-Graham, L. and Storm, J. F. (1999). The role of BK-type Ca^{2+}-dependent K^+ channels in spike broadening during repetitive firing in rat hippocampal pyramidal cells. *J. Physiol.* **521**, 135-146.

Sheng, Z. H., Rettig, J., Takahashi, M. and Catterall, W. A. (1994). Identification of a syntaxin-binding site on N-type calcium channels. *Neuron* **13**, 1303-1313.

Sochivko, D., Chen, J., Becker, A. and Beck, H. (2003). Blocker-resistant Ca^{2+} currents in rat CA1 hippocampal pyramidal neurons. *Neuroscience* **116**, 629-638.

Storm, J. F. (1987). Action potential repolarization and a fast after-hyperpolarization in rat hippocampal pyramidal cells. *J. Physiol.* **385**, 733-759.

Sun, X., Gu, X. Q. and Haddad, G. G. (2003). Calcium influx via L- and N-type calcium channels activates a transient large-conductance Ca^{2+}-activated K^+ current in mouse neocortical pyramidal neurons. *J. Neurosci.* **23**, 3639-3648.

Vergara, C., Latorre, R., Marrion, N. V. and Adelman, J. P. (1998). Calcium-activated potassium channels. *Curr. Opin. Neurobiol.* **8**, 321-329.

Wanner, S. G., Koch, R. O., Koschak, A., Trieb, M., Garcia, M. L., Kaczorowski, G. J. and Knaus, H. G. (1999). High-conductance calcium-activated potassium channels in rat brain: pharmacology, distribution, and subunit composition. *Biochemistry* **38**, 5392-5400.

Westenbroek, R. E., Hell, J. W., Warner, C., Dubel, S. J., Snutch, T. P. and Catterall, W. A. (1992). Biochemical properties and subcellular distribution of a N-type calcium channel alpha 1 subunit. *Neuron* **9**, 1099-1115.

Wolfart, J. and Roeper, J. (2002). Selective coupling of T-type calcium channels to SK potassium channels prevents intrinsic bursting in dopaminergic midbrain neurons. *J. Neurosci.* **22**, 3404-3413.

Xia, X. M., Fakler, B., Rivard, A., Wayman, G., Johnson-Pais, T., Keen, J. E., Ishii, T., Hirschberg, B., Bond, C. T., Lutsenko, S. et al. (1998). Mechanism of calcium gating in small-conductance calcium-activated potassium channels. *Nature* **395**, 503-507.

Yasuda, T., Chen, L., Barr, W., McRory, J. E., Lewis, R. J., Adams, D. J. and Zamponi, G. W. (2004). Auxiliary subunit regulation of high-voltage activated calcium channels expressed in mammalian cells. *Eur. J. Neurosci.* **20**, 1-13.

Zamponi, G. W., Bourinet, E., Nelson, D., Nargeot, J. and Snutch, T. P. (1997). Crosstalk between G proteins and protein kinase C mediated by the calcium channel alpha1 subunit. *Nature* **385**, 442-446.

Journal of Cell Science